

Enantiotropic phase transition and twinning in 2,2,3,3,4,4-hexafluoropentane-1,5-diol

Jeong-Myeong Ha^a and Victor Young^{b*}^aDepartment of Chemical Engineering and Materials Science, University of Minnesota, 421 Washington Avenue SE, Minneapolis, MN 55455, USA, and^bDepartment of Chemistry, University of Minnesota, 207 Pleasant Street SE, Minneapolis, MN 55455, USA

Correspondence e-mail: vyoung@umn.edu

Received 4 May 2009

Accepted 29 June 2009

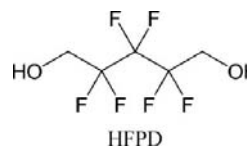
Online 11 July 2009

Four crystal structure determinations of 2,2,3,3,4,4-hexafluoropentane-1,5-diol (HFPD), $C_5H_6F_6O_2$, were conducted on a single specimen by varying the temperature. Two polymorphs of HFPD were found to be enantiotropically related as phases (I) and (II), both in the space group $P1$. These structures contain closely related $R_4^4(20)$ sheets. A structure determination was completed on form (Ia) at 283 K. Form (Ia) was then supercooled below the phase transition temperature at 279 to 173 K to give form (Ib) for a second structure determination. Metastable form (Ib) was transformed by momentary warming and recooling to give form (II) for a third structure determination at 173 K. Form (II) transformed to form (Ic) upon warming to 283 K. Enantiotropic phase transitions between phases (I) and (II) were confirmed with X-ray powder diffraction and differential scanning calorimetry. Form (Ia) was found as a twin by nonmerohedry by a reflection in (011). This twinning persists in all phases described. Additional twinning was found after the phase (I) to phase (II) transformation. These two additional twin components are related to the first pair by a 180° rotation about the (012) plane. This latter pair of twins persisted as the specimen was warmed back to form (Ic) at 283 K.

Comment

Enantiotropic phase transitions provide important information regarding the physical properties of the same material in different crystalline forms. These require two polymorphs that are each thermodynamically stable over a range of temperatures and pressures, where variation of either will lead to a phase transition to the other polymorph (Herbstein, 2006). Single-crystal-to-single-crystal transitions of crystalline solids have been observed for solid-state phase transitions of enantiotropic polymorphs (Caira *et al.*, 2004; Lim & Jeong,

2001; Asadov, 1967), pressure-dependent transitions between polymorphs (Fabbiani *et al.*, 2005), solid-state geometric isomerizations (Agmon & Kaftory, 1994), topochemical reactions (Enkelmann & Wegner, 1993), solid-state polymerizations (Okada *et al.*, 1994) and pseudo-polymorphic transitions of guest-inclusion compounds (Atwood *et al.*, 2002; Ananchenko *et al.*, 2006). There are reports of enantiotropic phase transitions accompanying a change of crystal system and space group while becoming twinned (Choe *et al.*, 2000; Colombo *et al.*, 2000; Guzei *et al.*, 2009; Jadzewski *et al.*, 2001; Reger *et al.*, 2001; Schweitzer *et al.* 2000). In the majority of these reports, the higher-temperature phase is also the higher-symmetry minimal non-isomorphic supergroup of the pair, while the lower-temperature phase becomes twinned in a maximal non-isomorphic subgroup. The present study is quite different, because there is no change in symmetry as the phase (I) to phase (II) transition occurs, but rather a sliding of the two unique diol molecules within the unit cell to the other polymorphic form.



The material of interest in this study, 2,2,3,3,4,4-hexafluoropentane-1,5-diol (HFPD), has been used as a reagent to prepare fluorinated polymers and as a precursor to cyclic and acyclic polyfluorosiloxanes (Johncock & Hewins, 1975; Elias *et al.*, 1994; Adhikari *et al.*, 1999; Patel *et al.*, 1994). The solid-state chemistry of fluorocarbons has been a subject of interest because of their unique properties in molecular solids (Reichenbacher *et al.*, 2005). HFPD has also been crystallized within the channels of nanoporous matrices (Ha *et al.*, 2005), where the initial report of the cell constants for both HFPD phases was presented.

Displacement ellipsoid drawings of all four structure determinations are shown in Fig. 1. All C—C, C—O and C—F distances of the two unique HFPD molecules appear to be in normal ranges for all four structure determinations presented here. However, the basic structural features of these two HFPD polymorphs are unique among reported diol structures (Allen, 2002). The space group for both is $P1$, with $Z = 2$ and $Z' = 2$. The molecules form a network of O—H...O hydrogen bonds through intersecting C(2) and C(8) chains that lead to $R_4^4(20)$ layers (Bernstein *et al.*, 1995; Etter, 1990; Etter *et al.*, 1990; Grell *et al.*, 1999). Both phases exhibit strong pseudo-symmetry as a pseudo- c -glide reflection perpendicular to the a -axis and pseudo-twofold symmetry perpendicular to the layers.

Initial twinned-crystal diffraction studies (not presented here) suggested the phase transition temperature was below the 283 K used for forms (Ia) and (Ic), and above the 173 K used for form (Ib) and (II). This was later confirmed by other means (see below). The packing diagrams for forms (Ib) and (II) at 173 K are shown in Fig. 2. The crystal structures of both phases (I) and (II) of HFPD are composed of stacked mol-

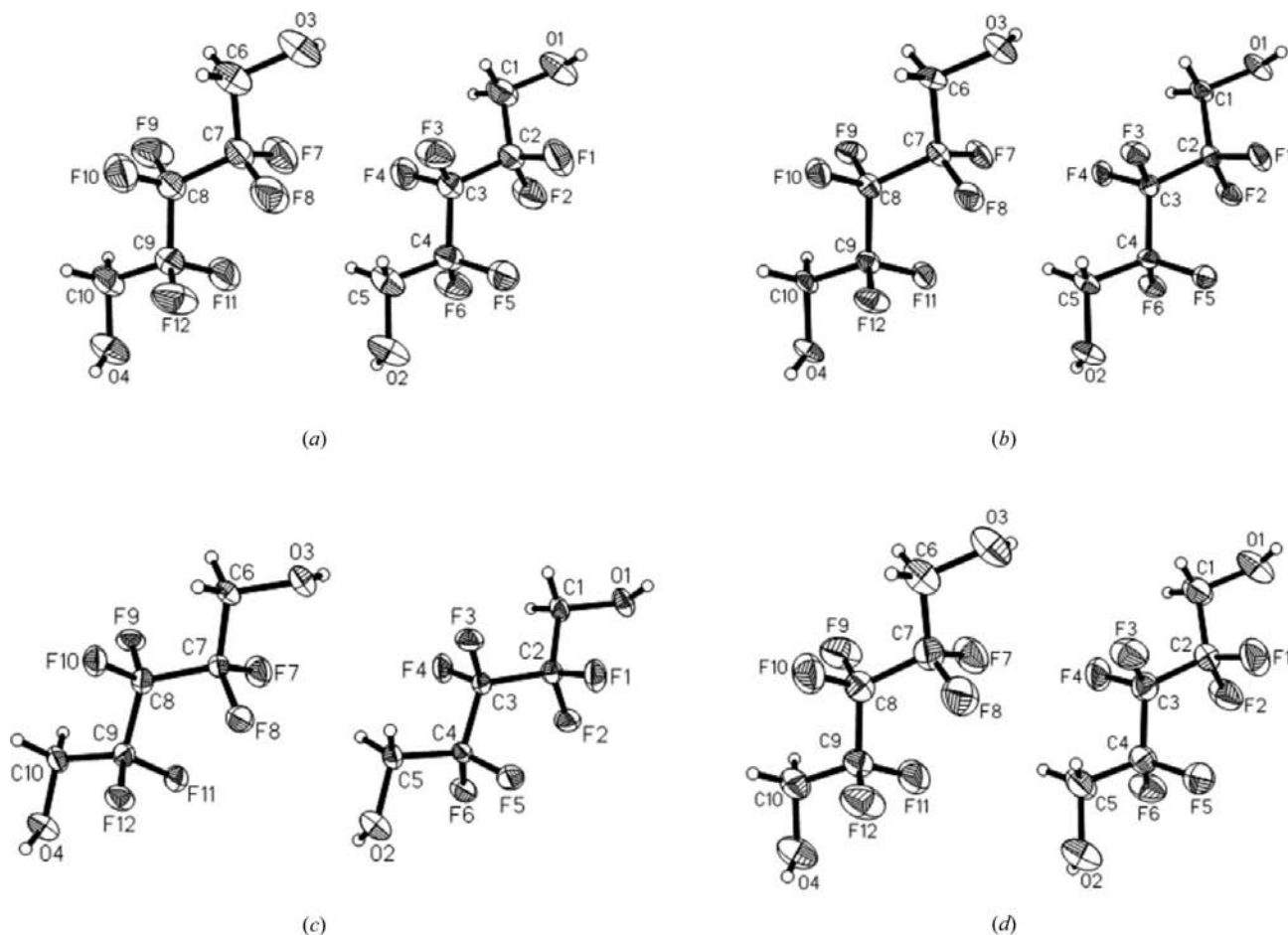


Figure 1

Views of the two independent molecules of each of the four forms of HFPD, showing the atom-numbering schemes, viz. (a) (Ia) at 283 K, (b) (Ib) at 173 K, (c) (II) at 173 K and (d) (Ic) at 283 K. Displacement ellipsoids are drawn at the 50% probability level and H atoms are shown as small spheres of arbitrary radii. Both unique molecules are shown in the same relative orientation for phases (I) and (II), as viewed along the [100] axis.

ecular sheets. These sheets, parallel to the (012) planes of each polymorph, have in-plane hydrogen bonding between primary hydroxyl groups. The hydrogen bonds, along with corrected H-atom positions based on normalized O—H distances, are presented in Table 1. The hydrogen-bonding network forms a rigid substructure that does not appear to change appreciably throughout the course of the study. Hydrogen bonds are reported with both distances and angles derived from riding O-bound H-atom positions (Sheldrick, 2008) and with normalized H-atom positions (Thalladi *et al.*, 1998). The only minor differences are observed as slightly shorter normalized $D\cdots A$ and $H\cdots A$ distances for forms (Ib) and (II), both at 173 K. The phase transition does not impose any substantial change on the hydrogen-bonding scheme, even though the unit cell undergoes a radical change.

The torsion angle analyses for each HFPD backbone are presented in Table 2. These vary considerably from planar zigzag hydrocarbon chains, where the expected values are approximately 180° (Dunitz, 2004). There are two types in this list. The first type incorporates the O atom of a hydroxyl group, a $-\text{CH}_2-$ group and the two adjacent $-\text{CF}_2-$ groups. The other type has a $-\text{CH}_2-$ group and three adjacent $-\text{CF}_2-$ groups. The average O—C—C—C torsion angle is $176.9(11)^\circ$,

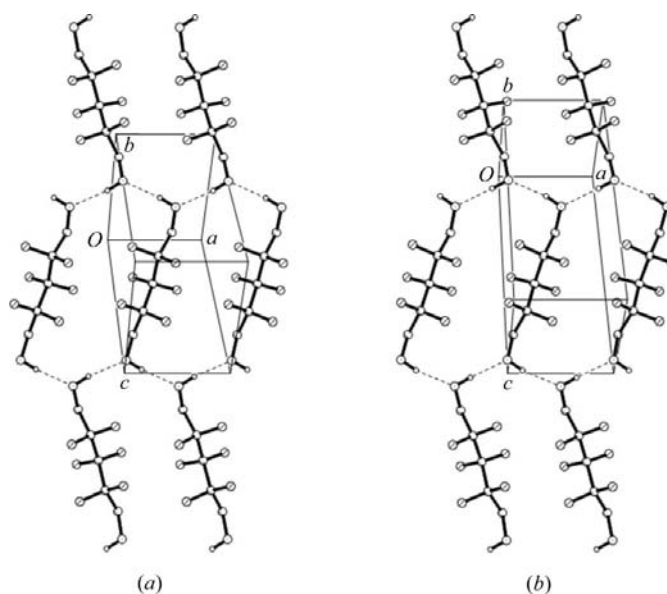


Figure 2

Packing diagrams for (a) form (Ib) and (b) form (II), both at 173 K, viewed with respect to the (012) plane and with the [100] axis parallel to the horizontal axis. The hydrogen-bonding network (dashed lines) is preserved through the phase transition.

while the average C—C—C—C torsion angle is 169.1 (15)°. Each of the two unique molecules is twisted by a different angle, averaging 25.7 (5) and 30.6 (12)° for respective molecules over the four structures presented here. This implies each HFPD molecule is twisted considerably from the aforementioned zigzag hydrocarbon chains. This twisting imposes chirality on each HFPD molecule. Given the presence of the pseudo-glide reflection operation and the two unique HFPD molecules in the unit cell, each HFPD molecule is a pseudo-enantiomer of the other. While respective molecules have about a 5° difference in the twist of the diol fragments, the weighted r.m.s. deviations for superposition of the enantiomers for all non-H atoms are 0.0393 for (Ia), 0.0474 for (Ib), 0.0399 for (II) and 0.0387 Å for (Ic).

The hydroxyl groups for phases (I) and (II) are effectively enclosed within the substructure, preventing nonbonded contacts with any F atoms. Similarly, the F atoms only take part in nonbonded contacts with C—F F atoms and C—H H atoms. This is strikingly similar to the property of mutual phobicity between fluorocarbons and hydrocarbons as described by Dunitz (2004). These functional groups tend to segregate within crystal structures when no overriding structural feature imposes an unfavorable contact. It appears the same reasoning is applicable to HFPD, which has the three different functional groups of hydroxyl, hydrocarbon and fluorocarbon.

While nonbonded contacts between hydroxyl groups and both hydrocarbon and fluorocarbon groups are surprisingly absent due to the efficient packing, there is a mixture of both F···F and C—H···F close contacts that appears to govern the enantiotropic phase transition. Table 3 presents all significant F···F nonbonded contacts throughout this study. Pairs of C—F bonds involved in single F···F intermolecular contacts are tracked through all structure determinations if at least one is less than 3.10 Å. All of these F···F intermolecular contacts shrink by 1.2 (4)% upon cooling of form (Ia) at 283 K to form (Ib) at 173 K, which follows the contraction of the unit-cell volume. The average F···F intermolecular contacts increase from 3.1 (5) Å in form (Ib) to 3.3 (6) Å in form (II). Two of the eight F···F intermolecular contacts in this group for both forms (Ib) and (II) are less than 2.90 Å, which is considered to be the limit for an F···F van der Waals contact (Rowland & Taylor, 1996; Bondi, 1964). Overall, the F···F intermolecular contacts are more favorable for form (II) at 173 K.

A similar situation is found for C—H···F close contacts in this study. Table 4 presents all significant C—H···F close contacts throughout the series. Form (Ia) at 283 K has three C—H···F close contacts less than 2.54 Å, one of which is less than 2.42 Å. C—H···F close contacts may be mildly stabilizing at distances greater than 2.54 Å (Rowland & Taylor, 1996), but rarely ever form (Dunitz & Taylor, 1997). In the few confirmed instances, the lower limit of a C—H···F close contact is approximately 2.36 Å when the hybridization of the C—H fragment is either *sp*² or *sp*³ (Thalladi *et al.*, 1998; Howard *et al.*, 1996). Upon cooling form (Ia) to the metastable form (Ib) at 173 K, these three close contacts decrease on average by 0.06 (2) Å. The shortest of the three C—H···F close contacts is within the van der Waals limit at 2.348 Å.

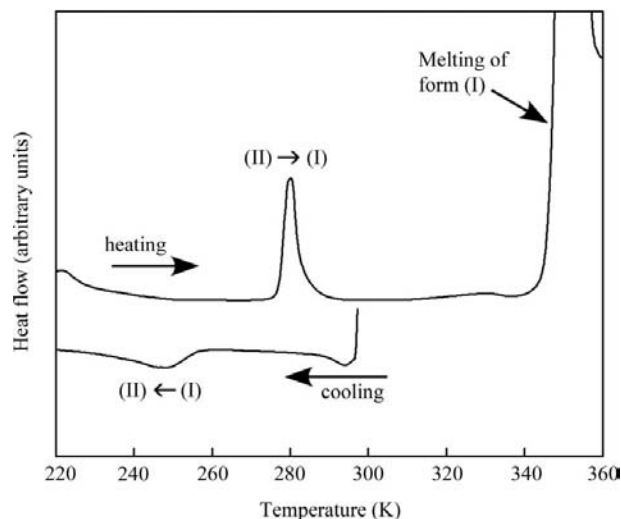


Figure 3

Differential scanning calorimetry analysis of HFPD in phase (I). The cooling cycle shows a more sluggish phase transition than the warming cycle.

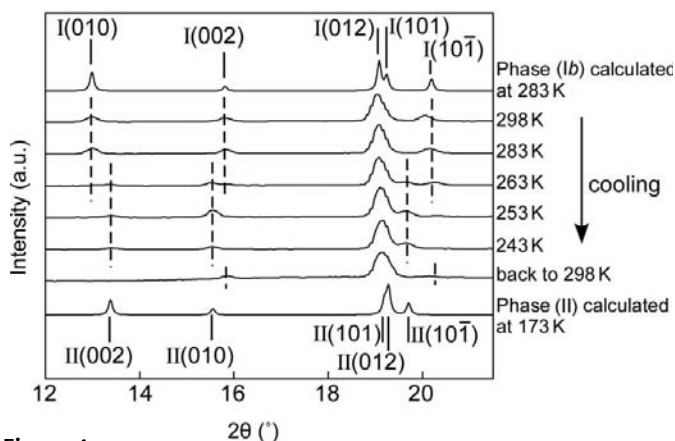
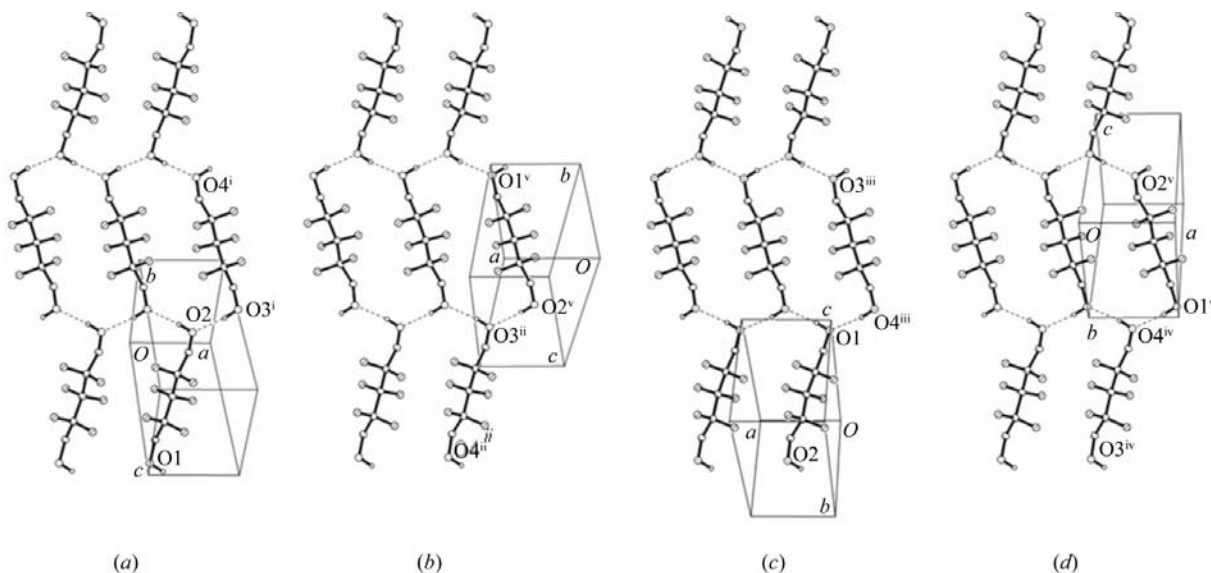


Figure 4

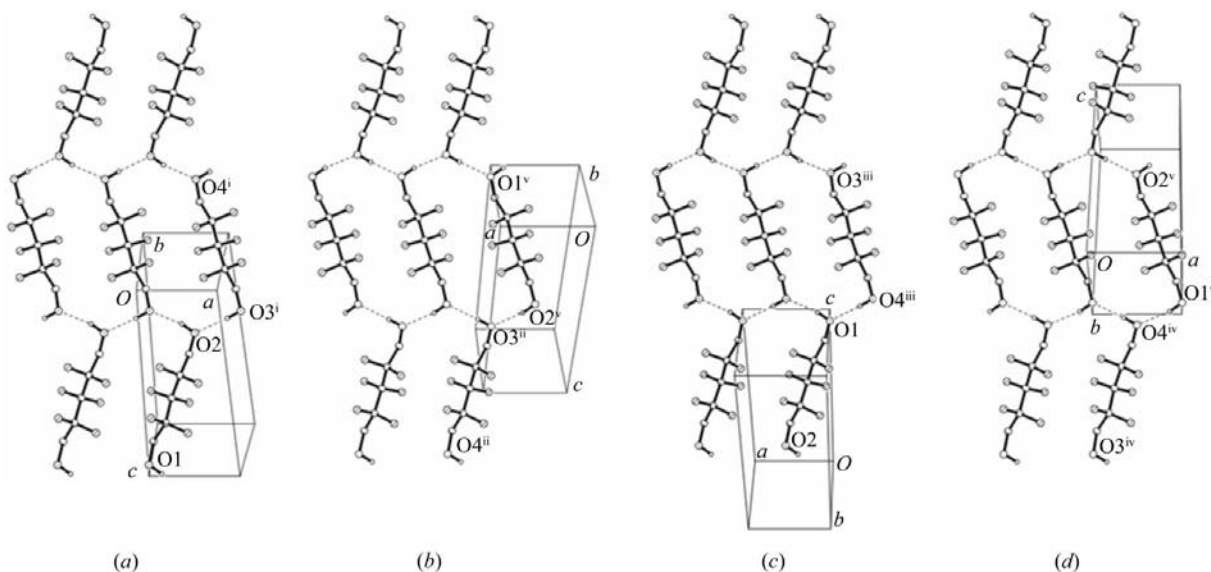
Temperature-dependent X-ray powder diffraction study of the phase (I) to phase (II) transition. Phase (I) persists from 283 to 263 K, then transforms completely to phase (II). Warming to 298 K restores HFPD to phase (I). Major calculated reflection positions for phase (I) (top) and phase (II) (bottom) are shown.

These C—H···F close contacts provide additional impetus for the enantiotropic phase transition to form (II). All C—H···F close contacts in form (II) are found in a narrower range of 2.535–2.628 Å, thereby avoiding any of the short C—H···F close contacts found in form (Ib). The result of the enantiotropic phase change is a slight increase in the density of form (II) of about 1.1% at this temperature.

The enantiotropic phase transition of HFPD was confirmed with differential scanning calorimetry (DSC) and powder X-ray diffraction (XRD). DSC analyses showed that the room-temperature stable phase (I) of HFPD transformed to the low-temperature stable phase (II) by cooling to 253 K, as exhibited in Fig. 3. Phase (II) reversibly transformed to phase (I) at 275–283 K by heating. Phase (I) melted to a liquid phase at 354 K. The enthalpy change of the phase transition of phase (II) to phase (I) was 0.44 (1) kJ mol^{−1}, while the enthalpy change on melting phase (I) to a liquid phase was

**Figure 5**

Phase (I) twin domains, showing (a) reference individual, (b) 180° rotation about the [100] axis plus inversion to enantiomorph or a reflection in the (011) plane, (c) 180° rotation about the (012) plane and (d) reflection in the (011) plane followed by a 180° rotation about the (012) plane. [Symmetry codes: (i) $x, y + 1, z$; (ii) $1 - x, -y - 1, -z$; (iii) $x - 1, y - 1, z + 1$; (iv) $-x, 1 - y, -z - 1$; (v) $-x, -y, -z$.]

**Figure 6**

Phase (II) twin domains, showing (a) reference individual, (b) 180° rotation about the [100] axis plus inversion to enantiomorph or a reflection in the (011) plane, (c) 180° rotation about the (012) plane and (d) reflection in the (011) plane followed by a 180° rotation about the (012) plane. [Symmetry codes: (i) $x, y + 1, z$; (ii) $1 - x, -y - 1, -z$; (iii) $x - 1, y - 1, z + 1$; (iv) $-x, 1 - y, -z - 1$; (v) $-x, -y, -z$.]

29.7 (3) kJ mol⁻¹. The observed enthalpy change for the solid-state phase transition is relatively small compared with other organic crystal structures (Yu *et al.*, 2000; Cingolani & Berchiesi, 1974; Petropavlov *et al.*, 1988; Steele *et al.*, 2002). Typical values of enthalpy changes for similar phase transitions fall in the range 1–10 kJ mol⁻¹, which is larger than the observed enthalpy change from phase (II) to (I) of HFPD. The small value of the enthalpy change can be attributed to the modest change in the crystal structure during the solid-state transition. Temperature-dependent XRD confirmed the phase transition between phases (I) and (II) that was observed in the single crystal of HFPD, as depicted in Fig. 4. Although the reflections of the (012) and (101) planes of phases (I) and (II)

are nearly indistinguishable by 2θ positions alone, disappearance of the 010, 002 and $10\bar{1}$ reflections of phase (I) and appearance of the corresponding reflections of phase (II) were clearly observed at 263–253 K during cooling from room temperature to 243 K. The reflections of phase (I) were obtained again when the crystalline powder was heated to room temperature.

It is of interest to compare these polymorphic HFPD diol structures with studies of the packing motifs of all diol structures (Taylor & Macrae, 2001). Both primary mono-alcohols and primary–primary diols are much more likely to form chain structures than ring structures. Chains are also favored for any diol with one primary alcohol. When considering all diols,

including secondary and tertiary, the frequencies of chain and ring structures are very similar. The HFPD polymorphs break this trend because these form two-dimensional sheets, despite being primary–primary diols. One point in common with primary–primary diol ring structures is that virtually all ring structures have four hydrogen bonds. A study of vicinal diols restates the observation that $Z' > 1$ structures are relatively common if each O atom is involved in more than one hydrogen bond (Brock, 2002).

The single specimen examined as part of this study, and a number of other unreported investigations of HFPD by the authors, were always twinned by nonmerohedry. These specimens were crystallized at temperatures higher than the phase transition, whether these were prepared by recrystallization from methanol, as was done in this study, or by sublimation. Diagrams of the twinning domains are presented in Fig. 5 for phase (I) and Fig. 6 for phase (II). Each twin domain depicted in these two diagrams is drawn with the (012) plane in the page and with the [100] axis parallel to the horizontal axis. The O atoms of each of the unique HFPD molecules are indicated, and the unit-cell axes are shown.

The two twin components of form (Ia) refined to a 0.724 (5):0.276 (5) ratio, with the second twin component corresponding to a 180° rotation about the [100] axis, as shown in Figs. 5(a) and 5(b). However, the assignment of the twin law does not take into account the possibility of racemic twinning in addition to this twin domain found by nonmerohedry. A twin law with only a 180° rotation about the [100] axis does not bring the composition plane into registry with the reference twin domain unless the enantiomorph is used. Therefore, the permutation of the twofold rotation in [100] and the inversion necessary to provide the enantiomorph is effectively a reflection in the (011) plane. Diffraction data acquired with molybdenum radiation prevents the determination of absolute configuration when F is the heaviest atom. However, this twin law provides for a seamless composition plane, or interface, between the respective twin domains. Form (Ib) can be isolated by carefully cooling the specimen to 173 K, which will preserve the same two twin domains as in form (Ia), but these refined to a 0.597 (5):0.403 (5) ratio. It appears that there is some conversion of the reference individual to the minor individual as the temperature is reduced. A momentary warming by blocking the cryostat flow and recooling causes the phase transition from form (Ib) to form (II). Form (II) contains the same two twin domains as form (Ib), as shown in Figs. 6(a) and 6(b), but two additional twin components are discovered, concomitant with the enantiotropic phase transition, as shown in Figs. 6(c) and 6(d). The ratio of twin components for form (II) is 0.339 (6):0.408 (6):0.141 (5):0.112 (4). It is presumed that the appearance of the third and fourth twin components is due to deformation in conjunction with the (Ib) to (II) phase transition. The relationship between twin component pairs 1/3 and 2/4 is a 180° rotation about the perpendicular to the (012) plane, thereby exploiting the twofold pseudosymmetry within the layer structure. The relationship between twin component pair 3/4 is the same as that between pair 1/2, described above. Finally, when form (II)

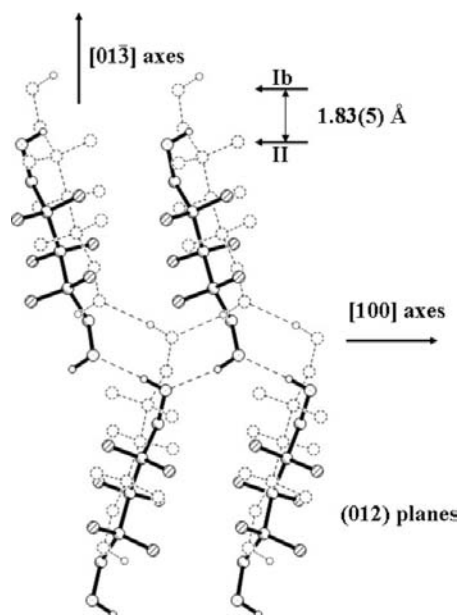


Figure 7

The superposition of (012) layers of (Ib) and (II), presented to illustrate the sliding of the layers during the enantiotropic phase transition of HFPD. Basal layers (not shown here) were overlaid to yield an r.m.s. deviation of 0.16 Å for respective pairs of O atoms. A composite image is shown, containing (012) layers for (Ib) and (II) above the basal layer, with the [100] axis horizontal and the [013] axis vertical. Molecules of form (Ib) are drawn with dashed bonds and molecules of form (II) are drawn with solid bonds. Each layer slides 1.83 (5) Å along the [013] axis in the (012) plane, based on the translation of respective pairs of O atoms in forms (Ib) and (II).

is warmed back to 283 K, all four twin domains present are retained in form (Ic) after the phase (II) to phase (I) transition occurs. The ratio of twin components for (Ic) is 0.333 (6):0.434 (6):0.110 (5):0.122 (4). These two additional twin domains present in (Ic) are shown in Figs. 5(c) and 5(d).

The phase transition between phases (I) and (II) is accomplished by a sliding of the (012) layers in the [013] direction, as shown in Fig. 7. The contraction of the unit cell in form (Ia) on cooling to form (Ib), coupled with several unfavorable close contacts in form (Ib), as discussed above, precipitates the phase transition to form (II), whereby all layers slide by approximately 1.83 (5) Å.

Experimental

HFPD (98% pure) was purchased from Aldrich (Milwaukee, Wisconsin, USA) and used without further purification. Twinned crystals of HFPD were grown by slow evaporation of a methanol solution under ambient conditions. A specimen was glued with epoxy cement to the tip of a 0.15 mm diameter glass fiber and mounted on a Bruker SMART 1000 CCD Platform diffractometer equipped with an Oxford Cryosystems Cryostream 600 cryostat (Cosier & Glazer, 1986). Form (Ia) was placed on the diffractometer at 283 K and the data collected. Form (Ib) was obtained by supercooling the metastable phase (I) at a rate of 1 K min⁻¹ to 173 K. This crystalline phase persisted throughout the data collection at 173 K. In order to obtain phase (II) at 173 K, the flow of the cryostat was blocked to allow the specimen to warm to room temperature for about 1 s, then the blockage was removed, which allowed the specimen to return to

173 K. Initial indexing revealed that the phase change to phase (II) had taken place. Data collection on phase (II) was completed, and then the cryostat was warmed at a rate of 1 K min⁻¹ to 283 K. The specimen returned to phase (I) and a final data collection on form (Ic) was completed.

DSC measurements were obtained from a fine-powdered sample of HFPD using a TA Instruments Q1000 DSC with a 5 K min⁻¹ temperature ramp. Temperature-dependent XRD data were collected from a finely powdered sample of HFPD on a Bruker GADDS microdiffractometer, with Cu K α radiation, coupled to a locally built cryostat with an Omega temperature controller.

Form (Ia) of HFPD

Crystal data

C₅H₆F₆O₂ $\gamma = 86.529 (3)^\circ$
 $M_r = 212.10$ $V = 380.41 (13) \text{ \AA}^3$
 Triclinic, *P*1 $Z = 2$
 $a = 4.9343 (10) \text{ \AA}$ Mo K α radiation
 $b = 6.8918 (14) \text{ \AA}$ $\mu = 0.23 \text{ mm}^{-1}$
 $c = 11.342 (2) \text{ \AA}$ $T = 283 \text{ K}$
 $\alpha = 81.943 (3)^\circ$ $0.35 \times 0.20 \times 0.17 \text{ mm}$
 $\beta = 85.847 (3)^\circ$

Data collection

Bruker SMART 1000 CCD 4125 measured reflections
 Platform diffractometer 1721 independent reflections
 Absorption correction: multi-scan 1419 reflections with $I > 2\sigma(I)$
 (TWINABS, Version 2008/1; $R_{\text{int}} = 0.030$
 Sheldrick, 2008)
 $T_{\text{min}} = 0.924$, $T_{\text{max}} = 0.962$

Refinement

$R[F^2 > 2\sigma(F^2)] = 0.034$ H-atom parameters constrained
 $wR(F^2) = 0.085$ $\Delta\rho_{\text{max}} = 0.18 \text{ e \AA}^{-3}$
 $S = 1.03$ $\Delta\rho_{\text{min}} = -0.17 \text{ e \AA}^{-3}$
 1721 reflections Absolute structure: Flack (1983),
 240 parameters with Friedel pairs merged
 3 restraints Flack parameter: 0.2 (9)

Form (Ib) of HFPD

Crystal data

C₅H₆F₆O₂ $\gamma = 85.640 (3)^\circ$
 $M_r = 212.10$ $V = 372.16 (15) \text{ \AA}^3$
 Triclinic, *P*1 $Z = 2$
 $a = 4.8848 (12) \text{ \AA}$ Mo K α radiation
 $b = 6.8723 (16) \text{ \AA}$ $\mu = 0.23 \text{ mm}^{-1}$
 $c = 11.259 (3) \text{ \AA}$ $T = 173 \text{ K}$
 $\alpha = 82.261 (3)^\circ$ $0.35 \times 0.20 \times 0.17 \text{ mm}$
 $\beta = 84.711 (3)^\circ$

Data collection

Bruker SMART 1000 CCD 3947 measured reflections
 Platform diffractometer 1686 independent reflections
 Absorption correction: multi-scan 1480 reflections with $I > 2\sigma(I)$
 (TWINABS, Version 2008/1; $R_{\text{int}} = 0.033$
 Sheldrick, 2008)
 $T_{\text{min}} = 0.923$, $T_{\text{max}} = 0.961$

Refinement

$R[F^2 > 2\sigma(F^2)] = 0.041$ H-atom parameters constrained
 $wR(F^2) = 0.122$ $\Delta\rho_{\text{max}} = 0.40 \text{ e \AA}^{-3}$
 $S = 1.04$ $\Delta\rho_{\text{min}} = -0.29 \text{ e \AA}^{-3}$
 1686 reflections Absolute structure: Flack (1983),
 240 parameters with Friedel pairs merged
 3 restraints Flack parameter: -0.3 (10)

Form (II) of HFPD

Crystal data

C₅H₆F₆O₂ $\gamma = 86.435 (4)^\circ$
 $M_r = 212.10$ $V = 367.98 (16) \text{ \AA}^3$
 Triclinic, *P*1 $Z = 2$
 $a = 4.8641 (12) \text{ \AA}$ Mo K α radiation
 $b = 5.7380 (14) \text{ \AA}$ $\mu = 0.24 \text{ mm}^{-1}$
 $c = 13.325 (3) \text{ \AA}$ $T = 173 \text{ K}$
 $\alpha = 82.814 (3)^\circ$ $0.35 \times 0.20 \times 0.17 \text{ mm}$
 $\beta = 87.274 (3)^\circ$

Data collection

Bruker SMART 1000 CCD 5181 measured reflections
 Platform diffractometer 1652 independent reflections
 Absorption correction: multi-scan 1289 reflections with $I > 2\sigma(I)$
 (TWINABS, Version 2008/1; $R_{\text{int}} = 0.050$
 Sheldrick, 2008)
 $T_{\text{min}} = 0.922$, $T_{\text{max}} = 0.961$

Refinement

$R[F^2 > 2\sigma(F^2)] = 0.054$ H-atom parameters constrained
 $wR(F^2) = 0.138$ $\Delta\rho_{\text{max}} = 0.39 \text{ e \AA}^{-3}$
 $S = 1.04$ $\Delta\rho_{\text{min}} = -0.39 \text{ e \AA}^{-3}$
 1652 reflections Absolute structure: Flack (1983),
 242 parameters with Friedel pairs merged
 3 restraints Flack parameter: -0.8 (14)

Form (Ic) of HFPD

Crystal data

C₅H₆F₆O₂ $\gamma = 86.562 (5)^\circ$
 $M_r = 212.10$ $V = 377.3 (2) \text{ \AA}^3$
 Triclinic, *P*1 $Z = 2$
 $a = 4.9215 (18) \text{ \AA}$ Mo K α radiation
 $b = 6.871 (3) \text{ \AA}$ $\mu = 0.23 \text{ mm}^{-1}$
 $c = 11.314 (4) \text{ \AA}$ $T = 283 \text{ K}$
 $\alpha = 81.973 (5)^\circ$ $0.35 \times 0.20 \times 0.17 \text{ mm}$
 $\beta = 85.839 (5)^\circ$

Data collection

Bruker SMART 1000 CCD 5825 measured reflections
 Platform diffractometer 1729 independent reflections
 Absorption correction: multi-scan 1200 reflections with $I > 2\sigma(I)$
 (TWINABS, Version 2008/1; $R_{\text{int}} = 0.030$
 Sheldrick, 2008)
 $T_{\text{min}} = 0.924$, $T_{\text{max}} = 0.962$

Refinement

$R[F^2 > 2\sigma(F^2)] = 0.049$ H-atom parameters constrained
 $wR(F^2) = 0.129$ $\Delta\rho_{\text{max}} = 0.27 \text{ e \AA}^{-3}$
 $S = 1.02$ $\Delta\rho_{\text{min}} = -0.30 \text{ e \AA}^{-3}$
 1729 reflections Absolute structure: Flack (1983),
 242 parameters with Friedel pairs merged
 3 restraints Flack parameter: 0.2 (14)

All reflection data had Friedel pairs merged. Aliphatic H atoms were treated as riding on the host C atoms, with C—H = 0.96 Å and $U_{\text{iso}}(\text{H}) = 1.2U_{\text{eq}}(\text{C})$ for forms (Ia) and (Ic), and with C—H = 0.98 Å and $U_{\text{iso}}(\text{H}) = 1.2U_{\text{eq}}(\text{C})$ for forms (Ib) and (II). Hydroxyl H atoms were initially located in difference Fourier maps and thereafter treated as idealized, torsionally refined on the host O atoms, with O—H = 0.82 Å and $U_{\text{iso}}(\text{H}) = 1.5U_{\text{eq}}(\text{O})$ for forms (Ia) and (Ic), and with O—H = 0.84 Å and $U_{\text{iso}}(\text{H}) = 1.5U_{\text{eq}}(\text{O})$ for forms (Ib) and (II).

For all four forms, data collection: SMART (Bruker, 1997); cell refinement: SAINT (Bruker, 2007); data reduction: SHELXL97 (Sheldrick, 2008); program(s) used to solve structure: SHELXS97

Table 1

Hydrogen-bond geometry of HFPD (Å, °), including H atoms at normalized positions for forms (Ia), (Ib), (II) and (Ic).

The first row of data for each hydrogen bond is based on riding H-atom positions, and the second row on a *D*—H bond length extended to 0.983 Å along the *D*—H vector obtained from the refinement.

<i>D</i> —H... <i>A</i>	<i>D</i> —H	H... <i>A</i>	<i>D</i> ... <i>A</i>	<i>D</i> —H... <i>A</i>
Form (Ia)				
O1—H1A...O4 ⁱ	0.82	1.93	2.740 (3)	168
	0.983	1.773		167
O2—H2A...O3 ⁱⁱⁱ	0.82	1.93	2.742 (4)	169
	0.983	1.772		168
O3—H3A...O2 ⁱⁱⁱ	0.82	1.96	2.758 (4)	165
	0.983	1.800		164
O4—H4A...O1 ^{iv}	0.82	1.94	2.746 (4)	166
	0.983	1.787		164
Form (Ib)				
O1—H1A...O4 ⁱ	0.84	1.89	2.717 (4)	169
	0.983	1.747		169
O2—H2A...O3 ⁱⁱⁱ	0.84	1.90	2.732 (5)	169
	0.983	1.762		168
O3—H3A...O2 ⁱⁱⁱ	0.84	1.91	2.740 (5)	171
	0.983	1.766		170
O4—H4A...O1 ^{iv}	0.84	1.91	2.733 (4)	166
	0.983	1.773		165
Form (II)				
O1—H1A...O4 ⁱ	0.84	1.93	2.746 (6)	163
	0.983	1.798		161
O2—H2A...O3 ⁱⁱⁱ	0.84	1.89	2.714 (6)	167
	0.983	1.751		166
O3—H3A...O2 ⁱⁱⁱ	0.84	1.93	2.733 (6)	160
	0.983	1.796		158
O4—H4A...O1 ^{iv}	0.84	1.90	2.736 (6)	175
	0.983	1.756		175
Form (Ic)				
O1—H1A...O4 ⁱ	0.82	1.93	2.736 (5)	169
	0.983	1.766		168
O2—H2A...O3 ⁱⁱⁱ	0.82	1.93	2.728 (6)	166
	0.983	1.768		165
O3—H3A...O2 ⁱⁱⁱ	0.82	1.96	2.756 (6)	164
	0.983	1.802		163
O4—H4A...O1 ^{iv}	0.82	1.96	2.741 (6)	158
	0.983	1.814		156

Symmetry codes: (i) *x*, *y* − 1, *z* + 1; (ii) *x* − 1, *y* + 1, *z*; (iii) *x*, *y* − 1, *z*; (iv) *x* + 1, *y* + 1, *z* − 1.

Table 2

Selected torsion angles (°) for both unique HFPD molecules in forms (Ia), (Ib), (II) and (Ic).

	(Ia)	(Ib)	(II)	(Ic)
O1—C1—C2—C3	175.6 (3)	175.6 (3)	178.4 (5)	176.0 (5)
C1—C2—C3—C4	169.1 (3)	169.1 (3)	169.7 (5)	169.2 (4)
C2—C3—C4—C5	171.5 (3)	171.5 (3)	170.3 (5)	171.1 (5)
C3—C4—C5—O2	178.3 (3)	178.2 (3)	175.2 (5)	178.4 (4)
O3—C6—C7—C8	−176.4 (3)	−176.2 (4)	−177.4 (5)	−176.7 (4)
C6—C7—C8—C9	−168.9 (3)	−168.9 (3)	−167.6 (5)	−169.1 (5)
C7—C8—C9—C10	−167.6 (3)	−167.0 (4)	−166.9 (5)	−167.8 (4)
C8—C9—C10—O4	−176.9 (3)	−176.5 (3)	−176.4 (5)	−177.4 (4)

(Sheldrick, 2008); program(s) used to refine structure: *SHELXL97*; molecular graphics: *SHELXL97*; software used to prepare material for publication: *SHELXL97*.

The authors acknowledge the MRSEC Program of the National Science Foundation (Award No. DMR-0212302) and

Table 3

Intermolecular F...F contacts (Å).

	(Ia)	(Ib)	(II)	(Ic)
F1...F2 ^{vi} /F2...F1 ^v	3.014 (4)	2.969 (4)	3.070 (5)	3.009 (6)
F2...F10 ^{viii} /F10...F2 ^{vii}	2.990 (3)	2.971 (4)	4.138 (4)	2.979 (5)
F3...F4 ^{vi} /F4...F3 ^v	2.922 (3)	2.881 (4)	2.860 (5)	2.913 (5)
F3...F5 ⁱⁱⁱ /F5...F3 ^{ix}	4.383 (3)	4.387 (3)	2.963 (5)	4.367 (4)
F4...F8 ^v /F8...F4 ^{vi}	2.905 (3)	2.877 (3)	4.173 (4)	2.903 (4)
F7...F8 ^v /F8...F7 ^{vi}	3.048 (4)	3.010 (4)	3.054 (6)	3.037 (6)
F9...F10 ^v /F10...F9 ^{vi}	2.893 (3)	2.841 (4)	2.836 (5)	2.881 (5)
F11...F12 ^v /F12...F11 ^{vi}	3.077 (4)	3.048 (4)	3.013 (5)	3.071 (6)

Symmetry codes: (iii) *x*, *y* − 1, *z*; (iv) *x* + 1, *y* + 1, *z* − 1; (v) *x* − 1, *y*, *z*; (vi) *x* + 1, *y*, *z*; (vii) *x* + 1, *y*, *z* − 1; (viii) *x* − 1, *y*, *z* + 1; (ix) *x*, *y* + 1, *z*.

Table 4

Intermolecular C—H...F contacts (Å) based on normalized H-atom positions.

The *D*—H bond length is extended to 0.983 Å along the *D*—H vector obtained from the refinement.

C—H...F	(Ia)	(Ib)	(II)	(Ic)
C1—H1B...F5 ⁱⁱⁱ	2.535	2.457	2.545	2.525
C1—H1C...F3 ^v	2.677	2.618	2.599	2.675
C5—H5A...F6 ^{vi}	2.888	2.737	2.570	2.809
C6—H6A...F12 ^{vi}	2.499	2.456	2.590	2.487
C6—H6B...F9 ^{vi}	2.752	2.683	2.628	2.730
C10—H10A...F10 ^v	2.711	2.639	2.564	2.709
C10—H10B...F2 ^{vii}	2.416	2.348	2.535	2.394

Symmetry codes: (iii) *x*, *y* − 1, *z*; (v) *x* − 1, *y*, *z*; (vi) *x* + 1, *y*, *z*; (vii) *x* + 1, *y*, *z* − 1.

the University of Minnesota for support. Twinned crystal data were collected at the X-ray Crystallographic Laboratory in the Department of Chemistry. DSC measurements were obtained in the Polymer Characterization Facility in the Department of Chemical Engineering and Materials Science. Powder XRD measurements were made in the Institute of Technology Characterization Facility. The authors thank Professor Doyle Britton (emeritus) and Dr Michael D. Ward (New York University) for helpful discussions.

Supplementary data for this paper are available from the IUCr electronic archives (Reference: GZ3166). Services for accessing these data are described at the back of the journal.

References

- Adhikari, R., Gunatillake, P. A., McCarthy, S. J. & Meijs, G. F. (1999). *J. Appl. Polym. Sci.* **74**, 2979–2989.
- Agmon, I. & Kaftory, M. (1994). *J. Appl. Cryst.* **27**, 146–150.
- Allen, F. H. (2002). *Acta Cryst.* **B58**, 380–388.
- Ananchenko, G. S., Udachin, K. A., Dubes, A., Ripmeester, J. A., Perrier, T. & Coleman, A. W. (2006). *Angew. Chem. Int. Ed.* **45**, 1585–1588.
- Asadov, Yu. G. (1967). *Kristallografiya*, **12**, 616–619.
- Atwood, J. L., Barbour, L. J., Jerga, A. & Schottel, B. L. (2002). *Science*, **298**, 1000–1002.
- Bernstein, J., Davis, R. A., Shimon, L. & Chang, N.-L. (1995). *Angew. Chem. Int. Ed.* **34**, 1555–1573.
- Bondi, A. (1964). *J. Phys. Chem.* **68**, 441–451.
- Brock, C. P. (2002). *Acta Cryst.* **B58**, 1025–1031.
- Bruker (1997). *SMART*. Version 5.054. Bruker AXS Inc., Madison, Wisconsin, USA.
- Bruker (2007). *SAINT*. Version 7.34A. Bruker AXS Inc., Madison, Wisconsin, USA.

- Caira, M. R., Foppoli, A., Sangalli, M. E., Zema, L. & Giordano, F. (2004). *J. Therm. Anal. Calorim.* **77**, 653–662.
- Choe, W., Pecharsky, V. K., Pecharsky, A. O., Gschneidner, K. A. Jr, Young, V. G. Jr & Miller, G. J. (2000). *Phys. Rev. Lett.* **84**, 4617–4620.
- Cingolani, A. & Berchiesi, G. (1974). *J. Therm. Anal.* **6**, 87–90.
- Colombo, D. G., Young, V. G. Jr & Gladfelter, W. L. (2000). *Inorg. Chem.* **39**, 4621–4624.
- Cosier, J. & Glazer, A. M. (1986). *J. Appl. Cryst.* **19**, 105–107.
- Dunitz, J. D. (2004). *ChemBioChem*, **5**, 614–621.
- Dunitz, J. D. & Taylor, R. (1997). *Chem. Eur. J.* **3**, 89–98.
- Elias, A. J., Hope, H., Kirchmeier, R. L. & Shreeve, J. M. (1994). *Inorg. Chem.* **33**, 415–418.
- Enkelmann, V. & Wegner, G. (1993). *J. Am. Chem. Soc.* **115**, 10390–10391.
- Etter, M. C. (1990). *Acc. Chem. Res.* **23**, 120–126.
- Etter, M. C., MacDonald, J. C. & Bernstein, J. (1990). *Acta Cryst. B* **46**, 256–262.
- Fabbiani, F. P. A., Allan, D. R., Parsons, S. & Pulham, C. R. (2005). *CrystEngComm*, **7**, 179–186.
- Flack, H. D. (1983). *Acta Cryst. A* **39**, 876–881.
- Grell, J., Bernstein, J. & Tinhofer, G. (1999). *Acta Cryst. B* **55**, 1030–1043.
- Guzei, I. A., Mitra, A. & Spencer, L. A. (2009). *Cryst. Growth Des.* **9**, 2287–2292.
- Ha, J.-M., Hillmyer, M. A. & Ward, M. D. (2005). *J. Phys. Chem.* **109**, 1392–1399.
- Herbstein, F. H. (2006). *Acta Cryst. B* **62**, 341–383.
- Howard, J. A. K., Hoy, V. J., O'Hagan, D. & Smith, G. T. (1996). *Tetrahedron*, **52**, 12613–12622.
- Jadzewski, B. A., Holland, P. L., Pink, M., Young, V. G. Jr, Spencer, D. J. E. & Tolman, W. B. (2001). *Inorg. Chem.* **40**, 6097–6107.
- Johncock, P. & Hewins, M. A. H. (1975). *J. Polym. Sci. Polym. Chem. Ed.* **13**, 807–814.
- Lim, A. R. & Jeong, S.-Y. (2001). *Physica B*, **304**, 79–85.
- Okada, S., Matsuda, H., Otsuka, M., Kikuchi, N., Hayamizu, K., Nakanishi, H. & Kato, M. (1994). *Bull. Chem. Soc. Jpn.*, **67**, 455–461.
- Patel, N. R., Chen, J., Zhang, Y. F., Kirchmeier, R. L. & Shreeve, J. M. (1994). *Inorg. Chem.* **33**, 5463–5470.
- Petropavlov, N. N., Tsygankova, I. G. & Teslenko, L. A. (1988). *Sov. Phys. Crystallogr.* **33**, 853–855.
- Reger, D. L., Little, C. A., Young, V. G. Jr & Pink, M. (2001). *Inorg. Chem.* **40**, 2870–2874.
- Reichenbacher, K., Süß, H. I. & Hulliger, J. (2005). *Chem. Soc. Rev.* **34**, 22–30.
- Rowland, R. S. & Taylor, R. (1996). *J. Phys. Chem.* **100**, 7384–7391.
- Schweitzer, J. W., Martinson, L. S., Baensiger, N. C., Swenson, D. C., Young, V. G. Jr & Guzei, I. (2000). *Phys. Rev. B*, **62**, 12792–12799.
- Sheldrick, G. M. (2008). *Acta Cryst. A* **64**, 112–122.
- Steele, W. V., Chirico, R. D., Cowell, A. B., Knipmeyer, S. E. & Nguyen, A. (2002). *J. Chem. Eng. Data*, **47**, 725–739.
- Taylor, R. & Macrae, C. F. (2001). *Acta Cryst. B* **57**, 815–827.
- Thalladi, V. R., Weiss, H.-C., Bläser, D., Boese, R., Nangia, A. & Desiraju, G. R. (1998). *J. Am. Chem. Soc.* **120**, 8702–8710.
- Yu, L., Stephenson, G. A., Mitchell, C. A., Bunnell, C. A., Snorek, S. V., Bowyer, J. J., Borchardt, T. B., Stowell, J. G. & Byrn, S. R. (2000). *J. Am. Chem. Soc.* **122**, 585–591.